Interpolation Based Local Postprocessing for Adaptive Finite Element Approximations in Electronic Structure Calculations

Jun Fang[1], Xingyu Gao[2], Xingao Gong[3], and Aihui Zhou[1]

[1] LSEC, Institute of Computational Mathematics and Scientific/Engineering Computing, Academy of Mathematics and Systems Science, Chinese Academy of Sciences, Beijing 100190, China,
`fangjun@lsec.cc.ac.cn; azhou@lsec.cc.ac.cn`

[2] HPCC, Institute of Applied Physics and Computational Mathematics, Beijing 100094, China,
`gao_xingyu@iapcm.ac.cn`

[3] Department of Physics, Fudan University, Shanghai 200433, China,
`xggong@fudan.edu.cn`

Summary. In this paper, we propose an interpolation based local postprocessing approach for finite element electronic structure calculations over locally refined hexahedral finite element meshes. It is shown that our approach is very efficient in finite element approximations of ground state energies.

Key words: adaptive finite element, eigenvalue, electronic structure, interpolation, Kohn–Sham equation, local postprocessing

1 Introduction

It is significant to obtain the ground state energy in the electronic structure study. In modern electronic structure calculations, the ground state energy is usually obtained from solving the Kohn–Sham equation [4, 17]. A general concern is the Kohn–Sham equation of a confined system posed on a bounded domain $\Omega \subset \mathbb{R}^3$:

$$\begin{cases} (-\frac{1}{2}\Delta + V_{eff}(\rho))\psi_i = \epsilon_i \psi_i, & \text{in } \Omega, \\ \psi_i = 0, & \text{on } \partial\Omega, \quad i = 1, \ldots, N_s, \end{cases} \tag{1}$$

where $\rho(\mathbf{r}) \equiv \sum_{i=1}^{N_s} f_i |\psi_i(\mathbf{r})|^2$ is the electron density, N_s the number of electron orbitals ψ_i with associated occupancy number f_i, and $V_{eff}(\rho)$ the so-called effective potential that is a nonlinear functional of ρ.

To solve nonlinear eigenvalue problem (1), a self-consistent approach such as DIIS (Direct Inversion Iterative Subspace) or Pulay's method in [22, 23] is required. As a result, the central computation in solving the Kohn–Sham equation is the repeated solution of the following type of linear eigenvalue problem:

$$\begin{cases} -\Delta u + Vu = \lambda u, & \text{in } \Omega, \\ u = 0, & \text{on } \partial\Omega, \end{cases} \tag{2}$$

where V is some effective potential. Since the electron density at the ground state decays exponentially [2, 13, 27], we may set Ω to be a cube in the computation. Note that even though V in (2) was relatively smooth in the pseudopotential setting, the eigenfunctions of (2) would vary rapidly in the neighborhood of the nuclei but be diffuse further away. Thus some efficient multi-resolution is significant for approximating eigenfunctions in the real space [4, 6, 20].

The multi-resolution can be achieved by adaptive finite element discretizations. Indeed, the preponderant strength of the finite element method lies in its ability to arrange local refinements in the regions where there are strong variations and high resolution is needed while treating the distant zones from nuclei at a coarser scale. We refer the reader to [4, 8, 9, 10, 21, 28, 33] and the references cited therein for the applications of finite element methods to electronic structure calculations. In this work, adaptive hexahedral finite elements will be studied for a better accuracy and efficiency on such a cubic domain [5, 11].

Once finite element eigenfunctions reach the self-consistent convergence, some postprocessing techniques are worth while to enhance the approximations when the extra cost is low. Indeed, the effectiveness of finite element postprocessing has been already shown in [8, 9, 10, 26]. In this paper we propose an interpolation based local postprocessing scheme for finite element quantum eigenvalue approximations and apply the approach to improve the ground state energy approximation. This scheme is derived from our understanding of the behavior of wavefunctions. For a quantum many-particle system, there is a general principle of locality or "nearsightedness" that the properties at one point may be considered independent of what happens at distant points [14, 16, 20]. And wavefunctions of a quantum many-particle system are somehow smooth and oscillate in the region where the system is located only [2, 15, 32]. Thus local higher order finite elements should be used (c.f., e.g., [8, 9, 10]). The computational complexity of higher order finite element discretizations, however, is larger than that of lower order finite element discretizations. To reduce the complexity, in this paper, we will propose some higher order interpolation approach for fast higher order finite element eigenvalue approximations. This approach is a local postprocessing on the lower order finite element approximations with little extra cost.

Now let us give some more details for an illustrative exhibition of the main idea in this paper. The trilinear finite element eigenfunctions are expanded by the basis of trilinear finite elements distributed on the locally refined mesh. In the case of the self-consistent convergence, we locate the father cell with eight children lying at the finest level of the hierarchy of grids. Based on trilinear finite element solutions on the children, a new eigenfunction approximation can be easily constructed as a triquadratic polynomial on this father cell. And the local accuracy enhancement of eigenfunctions in the high-resolution regions will effectively improve the approximations of the associated eigenvalues as well as ground state energies by Rayleigh quotients.

Our interpolation approach may be viewed as an averaging technique over adaptive finite element meshes while the existing averaging technique for quantum eigenvalue approximations in [26] is set for the gradient of eigenfunctions, in particular, employs some global projection. It is significant that our interpolation based local postprocessing is carried out only over the local domain where the molecular system is located. More notably, there are no auxiliary degrees of freedom needed by our postprocessing since the high-order interpolation is locally constructed over the selected father cells at the coarser level next to the finest. So, our approach is good at memory requirement and computation complexity. The theoretical tool for motivating this idea is the local error estimates for finite element approximations developed in [29, 31] (see also Sect. 2.1). We should mention that an interpolation global postprocessing is first introduced in [18] for finite element eigenvalue approximations over uniformly finite element meshes.

It is shown numerically that our scheme is a potentially efficient postprocessing technique for computing quantum eigenvalues (see Sect. 3.2). In fact, the computed electron density in the region of the system can be improved by the local high-order interpolation postprocessing. So it is expected that our approach would also benefit calculations of other quantum quantities.

The rest of this paper is organized as follows. In the next section, we first introduce our hexahedral finite element discretizations and then illustrate the local interpolation postprocessing theoretically and numerically. We present some applications to electronic structure calculations in Sect. 3 and finally we provide some concluding remarks.

2 Interpolation Based Finite Element Postprocessing

In this section, we shall first describe some basic notation and a finite element discretization for eigenvalue problem (2) and then introduce our local interpolation postprocessing, which will be supported by numerical experiments for a model example.

We shall use the standard notation for Sobolev spaces $W^{s,p}(\Omega)$ and their associated norms and seminorms (see, e.g., [1]). For $p = 2$, we denote $H^s(\Omega) = W^{s,2}(\Omega)$ and $H_0^1(\Omega) = \{v \in H^1(\Omega) : v|_{\partial\Omega} = 0\}$, where $v|_{\partial\Omega} = 0$ is in the sense of trace, $\|\cdot\|_{s,\Omega} = \|\cdot\|_{s,2,\Omega}$ and $\|\cdot\|_{\Omega} = \|\cdot\|_{0,2,\Omega}$. (In some places in this paper, $\|\cdot\|_{s,2,\Omega}$ should be viewed as piecewise defined if necessary.)

Throughout this paper, we shall use the letter C (with or without subscripts) to denote a generic positive constant which may stand for different values at its different occurrences. One basic assumption on the mesh is that the level difference of two adjacent cells cannot be more than one. For $D \subset \Omega_0 \subset \Omega$, we use the notation $D \subset\subset \Omega_0$ to mean that $\mathrm{dist}(\partial D \setminus \partial\Omega, \partial\Omega_0 \setminus \partial\Omega) > 0$.

Let $\Omega = (a,b)^3$ with $a, b \in \mathbb{R}$. Let $T^h(\Omega)$ consist of hexahedra whith edges parallel to x-axis, y-axis and z-axis respectively, where h is the mesh size. Define

$$S^h(\Omega) = \{v \in C(\bar{\Omega}) : v|_\tau \in Q_\tau \ \forall \tau \in T^h(\Omega)\}, \tag{3}$$

where $Q_\tau = \text{span}\{x^i y^j z^k : 0 \le i,j,k \le 1\}$. Set $S_0^h(\Omega) = S^h(\Omega) \cap H_0^1(\Omega)$. These are Lagrange finite element spaces. We refer the reader to [7, 29] (see also [24, 25]) for their basic properties that will be used in our analysis.

If $I_h : C(\bar{\Omega}) \longrightarrow S^h(\Omega)$ is the trilinear Lagrange finite element interpolation operator associated with $T^h(\Omega)$, then we derive from integration by parts that (see, e.g., [12, 19])

$$\left| \int_\tau \nabla(w - I_h w)\nabla v \right| \le C h_\tau^2 |w|_{3,\tau} |\nabla v|_{0,\tau} \ \ \forall v \in S^h(\Omega), \ \forall \tau \in T^h(\Omega), \tag{4}$$

where h_τ is the diameter of τ.

2.1 Finite Element Discretizations

A standard finite element discretization for (2) is: Find a pair of $(\lambda_h, u_h) \in \mathbb{R} \times S_0^h(\Omega)$ satisfying $\|u_h\|_{0,\Omega} = 1$ and

$$a(u_h, v) = \lambda_h (u_h, v) \ \ \forall v \in S_0^h(\Omega). \tag{5}$$

We use (λ_h, u_h) as an approximation to $(\lambda, u) \in \mathbb{R} \times H_0^1(\Omega)$, where (λ, u) is a solution of

$$a(u, v) = \lambda (u, v) \ \ \forall v \in H_0^1(\Omega) \tag{6}$$

with $\|u\|_{0,\Omega} = 1$ and

$$a(w, v) = \int_\Omega \frac{1}{2} \nabla w \nabla v + V w v \ \ \forall w, v \in H_0^1(\Omega).$$

If $V \in L^\infty(\Omega)$, then the associated exact eigenfunction $u \in H_0^1(\Omega) \cap H^2(\Omega)$. Thus we may assume that (see, e.g., [3])

$$|\lambda - \lambda_h| + h\|\nabla(u - u_h)\|_{0,\Omega} + \|u - u_h\|_{0,\Omega} \le Ch^2. \tag{7}$$

Let $P_h : H_0^1(\Omega) \longrightarrow S_0^h(\Omega)$ be the Galerkin projection defined by

$$a(w - P_h w, v) = 0 \ \ \forall v \in H_0^1(\Omega). \tag{8}$$

Then we have (see [30])

Proposition 1. *There holds*

$$\|P_h u - u_h\|_{1,\Omega} \le Ch^2. \tag{9}$$

2.2 Interpolation Based Local Postprocessing

Let Ω_0 be a subdomain of Ω. The following local superclose result can be derived from (4) and the local error estimation of finite element Galerkin approximations (see, e.g., [19])

Proposition 2. *Let $D \subset\subset \Omega_0$. If $u \in H_0^1(\Omega) \cap H^3(\Omega_0)$, then*

$$\|P_h u - I_h u\|_{1,D} \le Ch^2. \tag{10}$$

It is seen that we can define a triquadratic Lagrange interpolation Π_{2h} on any father cell $\Box$ that consists of 27 children elements in $T^h(\Omega)$. Let Ω_0 be covered by a group of father cells and aligned with $T^h(\Omega)$. Note that

$$\begin{aligned} \Pi_{2h} I_h &= \Pi_{2h}, \\ \|\nabla \Pi_{2h} v\|_{0,\Box} &\le \|\nabla v\|_{0,\Box} \quad \forall v \in S^h(\Omega), \\ \|\Pi_{2h} w - w\|_{1,\Box} &\le Ch^2 \|w\|_{3,\Box}. \end{aligned}$$

We obtain

$$\|\Pi_{2h} u_h - u\|_{1,D} \le Ch^2 \tag{11}$$

from Proposition 1, Proposition 2, and the identity

$$\Pi_{2h} u_h - u = \Pi_{2h}(u_h - P_h u) + \Pi_{2h}(P_h u - I_h u) + \Pi_{2h} u - u.$$

We may use some a Rayleigh quotient to get a new eigenvalue approximation λ^h as follows

$$\lambda^h = \frac{a(u^h, u^h)}{\| u^h \|_{0,\Omega}^2},$$

where

$$u^h = \begin{cases} \Pi_{2h} u_h & \text{, in } \bar{\Omega}_0, \\ u_h & \text{, in } \Omega \setminus \bar{\Omega}_0. \end{cases} \tag{12}$$

Indeed, our numerical experiments show that λ^h is much more accurate than λ_h even if Ω_0 is a part of Ω where local quadratic interpolation Π_{2h} can be carried out.

2.3 Quantum Harmonic Oscillator

For illustration, we consider an oscillator model, which is a simple problem in quantum mechanics:

$$-\frac{1}{2}\Delta u + \frac{1}{2}|x|^2 u = \lambda u, \qquad \text{in } \mathbb{R}^3. \tag{13}$$

The first eigenvalue of (13) is $\lambda = 1.5$ and is associated with the eigenfunction $u = \gamma e^{-\frac{|x|^2}{2}}$, where γ is a nonzero constant so that $\|u\|_{0,\mathbb{R}^3} = 1$.

In our experiments, we choose $\Omega = (-5.0, 5.0)^3$ as the computational domain, on which the zero Dirichlet boundary condition is imposed. We use a uniform mesh as the initial mesh. We carry out local refinements on subdomain $\Omega_0 = (-2.5, 2.5)^3$ by uniformly refining once and consider $D = (1.25, 1.25)^3$. Let(λ_h, u_h), (λ^h, u^h) be the trilinear finite element approximation to (λ, u) and the interpolation postprocessing eigenpair, respectively. Define

$$e_h = |\lambda_h - \lambda| \, , \; e^h = \left|\lambda^h - \lambda\right| .$$

$$\eta_h = \|\nabla(u_h - u)\|_{0,D} \, , \; \eta^h = \|\nabla(\Pi_{2h} u_h - u)\|_{0,D} \, .$$

Numerical results in Table 1 show the errors of the first eigenpair which supports our theory.

Table 1. Oscillator: interpolation on Ω_0.

Initial mesh size	η_h	Order(η_h)	e_h	η^h	Order(η^h)	e^h
$1/2^{-3} \times 10.0$	0.20743		0.03846	0.14364		0.01407
$1/2^{-4} \times 10.0$	0.10508	0.98114	0.00975	0.03265	2.13730	0.00141
$1/2^{-5} \times 10.0$	0.05269	0.99589	0.00244	0.00817	1.99868	0.00024
$1/2^{-6} \times 10.0$	0.02636	0.99918	0.00061	0.00205	1.99471	0.00005

3 Applications to Electronic Structure Calculations

Now we apply the interpolation based local postprocessing approach to solving Kohn–Sham equation (1), from which we see that highly accurate finite element approximations can be obtained over adaptive finite element meshes by using triquadratic interpolation postprocessing on each father cell of the coarser level next to the finest of the grid hierarchy.

3.1 Linearization of Kohn–Sham Equation

Since Kohn–Sham equation (1) is a nonlinear eigenvalue system, we need to linearize and solve it iteratively, which is called self-consistent field iteration (SCF). The SCF iteration is described as follows:

1. Given an initial electron density $\rho_{in}(\mathbf{r})$.
2. Compute $V_{eff}(\rho_{in})$ and solve

$$\begin{cases} (-\frac{1}{2}\Delta + V_{eff}(\rho_{in}))\psi_i = \epsilon_i \psi_i, & \text{in } \Omega, \\ \psi_i = 0, & \text{on } \partial\Omega, \\ \int_\Omega \psi_i \psi_j = \delta_{ij}, & i, j = 1, \ldots, N_s. \end{cases} \tag{14}$$

3. Set $\rho_{out} = \sum_{i=1}^{N_s} f_i |\psi_i(\mathbf{r})|^2$.

4. Compute the difference between ρ_{in} and ρ_{out}. If the difference is not small enough, “mix” density using Pulay’s method to obtain the new ρ_{in}, repeat from Step 2. Otherwise stop.

In our computation, Pulay’s method [22, 23] will be used. After self-consistent convergence is reached, we (carry out the postprocessing and) compute the total energy of the ground state [20]:

$$E_{tot} = \sum_{i=1}^{N_s} f_i \epsilon_i - \int_{\Omega} d\mathbf{r} V_{xc}(\mathbf{r})\rho(\mathbf{r}) - \frac{1}{2}\int_{\Omega}\int_{\Omega} \frac{\rho(\mathbf{r})\rho(\mathbf{r}')}{|\mathbf{r}-\mathbf{r}'|} + E_{xc}(\rho) + \frac{1}{2}\sum_{I,J=1,I\neq J}^{N_{nuclei}} \frac{Z_I Z_J}{|R_I - R_J|}, \tag{15}$$

where V_{xc} is the exchange-correlation potential, E_{xc} the exchange-correlation energy, $\epsilon_i (i = 1, \ldots, N_s)$ the eigenvalues, and R_I and Z_I^{ion} represent position and valence of the I-th atom, respectively.

3.2 Experiments

The initial electron density in our computation is constructed by some combination of the pseudo atomic obitals [11] and the adaptive refinement is done through the following a posteriori error estimators [8]:

$$h_\tau \|\nabla\rho\|_{0,\tau} \quad \forall\tau \in T^h(\Omega). \tag{16}$$

The mesh should be locally refined so as to meet the multi-resolution requirements (see Sect. 1). We locate father cells on the coarser level next to the finest of the grid hierarchy and carry out the triquadratic interpolation on these father cells. Our hexahedral mesh is well suited for this local interpolation: values of the trilinear finite element solutions on the 27 nodes are employed to determine the 27 coefficients of the required triquadratic Lagrange interpolating functions.

Figures 1, 2 and 3 are schematic figures illustrating the hexahedral discretizations before and after a local refinement around nuclei and the way to do the triquadratic interpolation. Figure 1 shows the standard hexahedral finite element discretizations and there is a nucleus within the dashed cell, for instance. Figure 2 gives the grid after refinement. The dashed subdomain has been divided into eight child cells. Figure 3 emphasizes those 27 nodes for the triquadratic Lagrange interpolation on the father cell.

After this “smoothing” of the eigenfunctions, we construct new eigenvalue approximations by the following Rayleigh quotients:

$$\epsilon_i = \frac{\frac{1}{2}\int_{\Omega} |\nabla u_i^h|^2 + \int_{\Omega} V_{eff}(\rho_{in})(u_i^h)^2}{\int_{\Omega}(u_i^h)^2}. \tag{17}$$

Consequently, the ground state total energy can be improved by these updated eigenvalues (c.f. (15)).

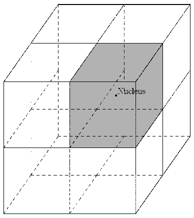

Fig. 1. Standard hexahedral FE discretizations with a nucleus in the dashed cell.

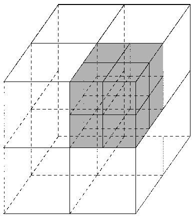

Fig. 2. Hexahedral mesh after local refinement on the dashed cell.

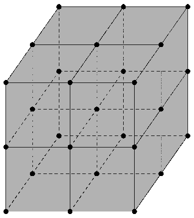

Fig. 3. 27 marked points for triquadratic interpolation on the father cell.

Our computing platform is a Dell Optiplex 755 (Intel Core Duo 2.6 GHz, 4 MB L2 cache, 2 GB memory), provided by the State Key Laboratory of Scientific and Engineering Computing (LSEC) of Chinese Academy of Sciences. Our programs are compiled with “g++ -O3” and run on a single core. The package ARPACK is employed as the eigensolver. The hexahedral grids are visualized by JaVis-1.2.3 developed by HPCC of Institute of Applied Physics and Computational Mathematics.

Benzene

Our computational domain for molecule benzene is $[-20.0, 20.0]^3$ and the adaptive finite element grids are generated on the basis of initial density and the a posteriori error estimators mentioned above. We see that the total energy decreases significantly after interpolation postprocessing. Note that the time of postprocessing is 5 s out of a total time of about 1 min.

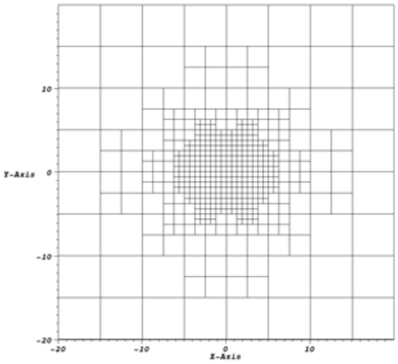

Fig. 4. A coarser mesh of C_6H_6 next to the finest mesh at $z = 0.0$ au.

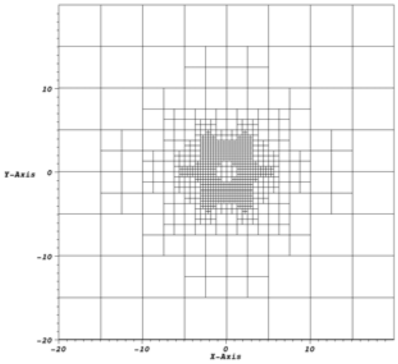

Fig. 5. The finest mesh of C_6H_6 at $z = 0.0$ au.

Table 2. Benzene: interpolation on a part of the father cells.

E_{tot}	Err. w.r.t SIESTA's	E_{tot}^{post}	Err. w.r.t SIESTA's
-37.03 au	1.5%	-37.58 au	0.053%

Table 3. Benzene: total CPU time and time for postprocessing.

Total CPU time	CPU time for postprocessing	Percentage
66.74 s	5.08 s	7.61%

Fullerene

To simulate the molecule C_{60}, we use $[-30.0, 16.0] \times [-23.0, 22.0] \times [-24.0, 21.0]$ as the computational domain. Table 4 shows that, after interpolation postprocessing on the father cells, we obtain a satisfactory approximation of the total energy. Besides, the computational cost is small compared to solving the linear eigenvalue problems. In this example, based on our choice of initial density, we achieve convergence after four self-consistent steps, and the time of postprocessing is 5 min out of a total time of about 80 min.

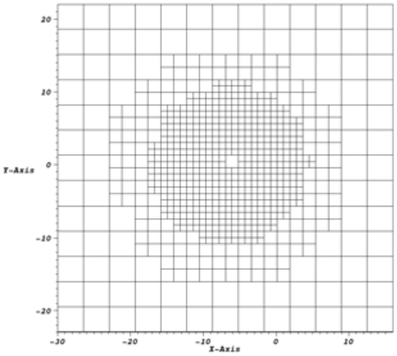

Fig. 6. A coarser mesh of C_{60} next to the finest mesh at $z = 0.0$ au.

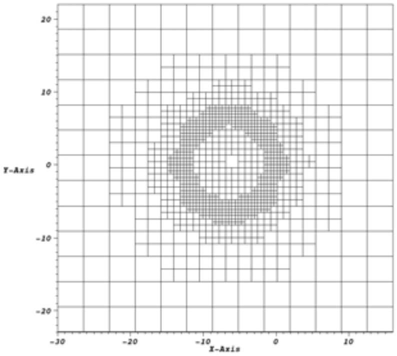

Fig. 7. The finest mesh of C_{60} at $z = 0.0$ au.

Table 4. Fullerene: interpolation on a part of the father cells.

E_{tot}	Err. w.r.t SIESTA's	E_{tot}^{post}	Err. w.r.t SIESTA's
-328.78 au	3.67%	-335.78 au	1.62%

Table 5. Fullerene: total CPU time and time for postprocessing.

Total CPU time	CPU time for postprocessing	Percentage
81 m 7.65 s	5 m 9.67 s	6.37%

4 Concluding Remarks

In this paper, we have proposed an interpolation based local postprocessing approach to adaptive finite element approximations in electronic structure calculations. It is shown by the theoretical analysis for linear eigenvalue problems and particularly successful applications to ground state energy calculations that this is a simple but powerful approach for highly accurate approximations. In our ongoing work, we apply this approach to computations of other quantum quantities of complex molecular systems.

Acknowledgement. This work was partially supported by the National Science Foundation of China under grants 10425105 and 10871198 and the National Basic Research Program under grant 2005CB321704. The authors would like to thank Dr. Xiaoying Dai, Prof. Lihua Shen, Mr. Zhang Yang, and Dr. Dier Zhang for their stimulating discussions and fruitful cooperations on electronic structure computations that have motivated this work.

References

1. R.A. Adams. *Sobolev Spaces*. Acadamic Press, New York, NY, 1975.
2. S. Agmon. *Lectures on the Exponential Decay of Solutions of Second-Order Elliptic Operators*. Princeton University Press, Princeton, NJ, 1981.
3. I. Babuska and J.E. Osborn. Finite element-Galerkin approximation of the eigenvalues and eigenvectors of self-adjoint problems. *Math. Comput.*, 52(186):275–297, 1989.
4. T.L. Beck. Real-space mesh techniques in density-functional theory. *Rev. Mod. Phys.*, 72:1041–1080, 2000.
5. J.R. Brauer. *What Every Engineer Should Know About Finite Element Analysis*. Marcel Decker Inc., New York, NY, 1993.
6. E.L. Briggs, D.J. Sullivan, and J. Bernholc. Real-space multigrid-based approach to large-scale electronic structure calculations. *Phys. Rev. B*, 54:14362–14375, 1996.
7. P.G. Ciarlet. *The Finite Element Method for Elliptic Problems*. North-Holland, Amsterdam, 1978.
8. X. Dai. *Adaptive and Localization Based Finite Element Discretizations for the First-Principles Electronic Structure Calculations*. PhD thesis, Academy of Mathematics and Systems Science, Chinese Academy of Sciences, Beijing, 2008.
9. X. Dai, L. Shen, and A. Zhou. A local computational scheme for higher order finite element eigenvalue approximations. *Int. J Numer. Anal. Model.*, 5:570–589, 2008.
10. X. Dai and A. Zhou. Three-scale finite element discretizations for quantum eigenvalue problems. *SIAM J. Numer. Anal.*, 46:295–324, 2008.
11. X. Gao. *Hexahedral Finite Element Methods for the First-Principles Electronic Structure Calculations*. PhD thesis, Academy of Mathematics and Systems Science, Chinese Academy of Sciences, Beijing, 2009.

12. X. Gao, F. Liu, and A. Zhou. Three-scale finite element eigenvalue discretizations. *BIT*, 48(3):533–562, 2008.
13. D. Gilbarg and N.S. Trudinger. *Elliptic Partial Differential Equations of Second Order*. Springer, Berlin, Heidelberg, third edition, 2001.
14. S. Goedecker. Linear scaling methods for the solution of Schrödinger's equation. In C. Le Bris, editor, Handbook of Numerical Analysis, volume X of Computational Chemistry. Elsevier, Amsterdam, 2003.
15. X. Gong, L. Shen, D. Zhang, and A. Zhou. Finite element approximations for Schrödinger equations with applications to electronic structure computations. *J. Comput. Math.*, 26: 310–323, 2008.
16. W. Kohn. Density functional and density matrix method scaling linearly with the number of atoms. *Phys. Rev. Lett.*, 76:3168–3171, 1996.
17. W. Kohn and L.J. Sham. Self-consistent equations including exchange and correlation effects. *Phys. Rev.*, 140(4A):A1133–A1138, 1965.
18. Q. Lin and Y. Yang. Interpolation and correction of finite elements (in Chinese). *Math. Pract. Theory*, (3):29–35, 1991.
19. Q. Lin and Q. Zhu. *The Preprocessing and Postprocessing for the Finite Element Method (in Chinese)*. Shanghai Scientific & Technical Publishers, Shanghai, 1994.
20. R.M. Martin. *Electronic Structure: Basic Theory and Practical Methods*. Cambridge University Press, Cambridge, 2004.
21. J.E. Pask and P.A. Sterne. Finite element methods in *ab initio* electronic structure calculations. *Model. Simul. Mater. Sci. Eng.*, 13:71–96, 2005.
22. P. Pulay. Convergence acceleration of iterative sequences in the case of scf iteration. *Chem. Phys. Lett.*, 73:393–398, 1980.
23. P. Pulay. Improved scf convergence acceleration. *J. Comput. Chem.*, 3:556–560, 1982.
24. A.H. Schatz and L.B. Wahlbin. Interior maximum-norm estimates for finite element methods. *Math. Comput.*, 31:414–442, 1977.
25. A.H. Schatz and L.B. Wahlbin. Interior maximum-norm estimates for finite element methods, Part II. *Math. Comput.*, 64:907–928, 1995.
26. L. Shen and A. Zhou. A defect correction scheme for finite element eigenvalues with applications to quantumn chemistry. *SIAM J. Sci. Comput.*, 28:321–338, 2006.
27. B. Simon. Schrödinger operators in the twentieth century. *J. Math. Phys.*, 41:3523–3555, 2000.
28. E. Tsuchida and M. Tsukada. Electronic-structure calculations based on the finite-element method. *Phys. Rev. B*, 52:5573–5578, 1995.
29. J. Xu and A. Zhou. Local and parallel finite element algorithms based on two-grid discretizations. *Math. Comput.*, 69:881–909, 2000.
30. J. Xu and A. Zhou. A two-grid discretization scheme for eigenvalue problems. *Math. Comput.*, 70:17–25, 2001.
31. J. Xu and A. Zhou. Local and parallel element algorithms for eigenvalue problems. *Acta. Math. Appl. Sin. Engl. Ser.*, 18:185–200, 2002.
32. H. Yserentant. On the regularity of the electronic Schrödinger equation in Hilbert space of mixed derivatives. *Numer. Math.*, 98:731–759, 2004.
33. D. Zhang, L. Shen, A. Zhou, and X. Gong. Finite element method for solving Kohn–Sham equations based on self-adaptive tetrahedral mesh. *Phys. Lett. A*, 372:5071–5076, 2008.